



Research Article

Andrea Prunotto, Wanda Maria Alberico, and Piotr Czerski*

Feynman diagrams and rooted maps

<https://doi.org/10.1515/phys-2018-0023>

Received Jul 21, 2017; accepted Jan 08, 2018

Abstract: The rooted maps theory, a branch of the theory of homology, is shown to be a powerful tool for investigating the topological properties of Feynman diagrams, related to the single particle propagator in the quantum many-body systems. The numerical correspondence between the number of this class of Feynman diagrams as a function of perturbative order and the number of rooted maps as a function of the number of edges is studied. A graphical procedure to associate Feynman diagrams and rooted maps is then stated. Finally, starting from rooted maps principles, an original definition of the genus of a Feynman diagram, which totally differs from the usual one, is given.

Keywords: Feynman Diagrams, Rooted maps, Many-body systems

PACS: 03.70.+k, 02.40.Pc

The problem of a correct and convenient counting of connected Feynman diagrams was often raised by Alfredo Molinari during his lectures in many-body physics. This paper took origin from his inquiries on the subject and is dedicated to his memory.

1 Introduction

Important progress has been made in recent years in developing the interplay between theoretical physics and graph theory (Floer [1–3], Fukaya [4–7], Schaeffer [8–13]). Mathematicians and physicists worked to combine theo-

ries of planar trees and rooted maps with the enumeration of Feynman diagrams for field theories, essentially quantum electrodynamics (QED), quantum gravity and quantum computing (Atiyah [14], Witten [15, 16], t’Hooft [17], De Wolf [18], Di Francesco [19]). The problem of counting Goldstone Diagrams has already been solved, Rossky and Karplus [20], but it is a rather difficult task to list all publications about Feynman diagrams counting. Here, we focus the attention on the combinatorial point of view studied in depth by Kucinskii and Sadovskii [21]. A graphical approach was followed for instance by Kleinert, Pelster, Kastening and Bachmann [22]. A more physical approach was followed by Riddell [23] and then by Brouder [24–26]. A strictly theoretical physics point of view in this field was explored instead by Cvitanović, Lautrup and Pearson [27], with conclusions identical to the ones of Arquès and Béraud [28, 29]. These results will be discussed in the following Sections.

The matter discussed here could be useful for automated Feynman diagram calculations, for example in the context of diagrammatic Monte Carlo [30] as well as for the recent attempts to automatize many-body perturbation theory calculations [31].

We shall present an original method to transform a Feynman diagram of the perturbative series expressing the single-particle propagator in many-body theory into a well defined rooted map. At variance with quantum electrodynamics, where Furry’s theorem [32] entails the cancellation of certain classes of diagrams, in the many-body approach the only cancellation occurring concerns the so-called disconnected diagrams: indeed in the many-body problem every connected diagram makes its contribution to the total amplitude (or Green’s function). This renders the counting of Feynman diagrams somewhat more difficult.

In last years, it has been discovered that the *number* of Feynman diagrams with regard to the perturbative order and the *number* of rooted maps as a function of edges (and regardless to genus and number of vertices) is the same. The strength of the numerical relation between Feynman diagrams and maps may suggest important links between general relativity and quantum mechanics, provided that we are able to trace, through the shape of the Feynman di-

***Corresponding Author: Piotr Czerski:** Institute of Computer Science, The Pedagogical University of Cracow, ul.Podchorążych 2, PL-30-084 Kraków, Poland; Email: piotr.czerski@up.krakow.pl
Andrea Prunotto: Dipartimento di Fisica dell’Università di Torino and Istituto Nazionale di Fisica Nucleare, Sezione di Torino, via P.Giuria 1, I-10125 Torino, Italy, E-mail: andrea.prunotto@gmail.com
Wanda Maria Alberico: Dipartimento di Fisica dell’Università di Torino and Istituto Nazionale di Fisica Nucleare, Sezione di Torino, via P.Giuria 1, I-10125 Torino, Italy, E-mail: alberico@to.infn.it



agram, the topological properties related to its opposing party rooted map.

The analytical and/or numerical evaluation of higher order terms in a perturbative series becomes more and more complicated: thus one could come to the conclusion that the exact enumeration of the corresponding Feynman diagrams is not so useful. Facing this doubt we would like to quote Cvitanović, Lautrup and Pearson [27]: “In trying to understand the behavior of field theory at large orders in perturbation theory, one finds that the number of diagrams contributing is an important effect. It is the cause of the combinatorial growth of amplitudes for superrenormalizable theories.” Hence we will proceed in the major task of this article, which is the investigation of a rule to enumerate Feynman many-body diagrams at various perturbative orders.

The paper is organized as follows: in Section 2 we shall briefly recall the main definitions and properties of topological maps, including the various enumerations of rooted maps (with or without taking into account specific characteristics of them). In Section 3, after a very short reckoning of the many-body single-particle Green’s function and its perturbative expression, we shall make explicit the connection between the corresponding Feynman diagrams and the rooted maps obtained from them. Moreover the topological properties of the considered Feynman diagrams, in particular the genus, will be discussed. Finally Section 4 will present our conclusions, leaving original details concerning the construction of the third (and higher) order Feynman diagrams to the Appendix.

2 Topological maps and rooted maps

A *map* is, roughly speaking, a partition of a closed, connected two-dimensional surface into simply connected polygonal regions by means of a finite number of simple curves (or edges) connecting pairs of points called vertices in such a way that the curves are disjoint from one another and from the vertices. The enumeration of *planar maps* (maps on the sphere or on the projective plane) has been extensively investigated since 1960, in particular by W. T. Tutte [33–35]. W. G. Brown then counted several types of maps on the projective plane and began investigating the torus, but did not obtain an explicit formula for counting maps on the torus [36–38].

Walsh and Lehman [39–41] presented the first census of maps on *oriented surfaces* of arbitrary genus in the early 70’s. A map was defined to be a *rooted* one (see section 2.1)

if one edge is distinguished, oriented and assigned a left and a right side. But since these authors worked on oriented (or, equivalently, orientable) surfaces, it suffices to distinguish and orient one edge-end because its left and right side are determined by the orientation of the surface. They considered two maps to be equivalent if they are related by an orientation preserving homeomorphism, according to Cairns [42] and Tutte [34], which leaves fixed the distinguished edge-end (called the *root*). We will use this work in order to show a graphical correspondence between maps and Feynman diagrams in the realm of quantum many-body theory.

At the end of the past century, Arquès and Béraud [28, 29] presented a different approach in the study of maps: they enumerated rooted maps without regard to genus - the genus of a map is essentially the genus of the embedding surface. They showed the existence of a new type of equation for the generating series of these maps enumerated with respect to edges and vertices: the Riccati’s equation. By means of Riccati’s equation Arquès and Béraud obtained a differential equation for the generating series of rooted trees regardless of the genus and as a function of edges which leads to a continued fraction for the generating series of rooted genus-independent trees and to a beautiful, unexpected relation between both previous generating series of trees and rooted maps. We will show that there exists a one to one relation between the number of rooted maps on orientable surfaces regardless to genus and with respect to edges and the number of Feynman diagrams for the one particle exact propagator as a function of perturbation order.

As we pointed out before, Walsh and Lehman [39–41] studied enumeration of rooted maps by genus, edges and vertices. Bender, Canfield and Robinson [43–46] studied in depth rooted maps on the torus and on the projective plane.

Moreover, many years ago J. Touchard [47] studied a problem of geometric configuration that actually corresponds to the enumeration on rooted maps, even though at the end of his work there seems to be a contradictory result. Work is presently going on on rooted maps (see for example Courcelle and Dussaux [48], Krikun and Malyshch [49–51], Shaeffer and Poulalhon [52–54], Jackson and Visentin [55], Yanpei [56]).

2.1 Definitions

2.1.1 Topological maps

A topological map M (see Figure 1) on an orientable surface¹ $\Sigma \subset \mathbf{R}^3$ is a partition of Σ in three sets:

- A finite set of points of Σ , called the *vertices* of M ;
- A finite set of simple open Jordan arcs² lying on Σ , disjoint in pairs³, whose extremes are vertices, denoted as the *edges* of the map;
- A finite set of *faces*. Each face is homeomorphic⁴ to an open disc. Its border is the union of vertices and edges.

Obviously we may build an orientation on Σ since we have chosen the surface Σ to be orientable. An oriented edge of the map is a *half-edge*. Evidently to each half-edge are associated its starting vertex and its ending vertex (and the underlying edge). The *genus* of the map M is the genus⁵ of the host surface (also known as *embedding surface*).

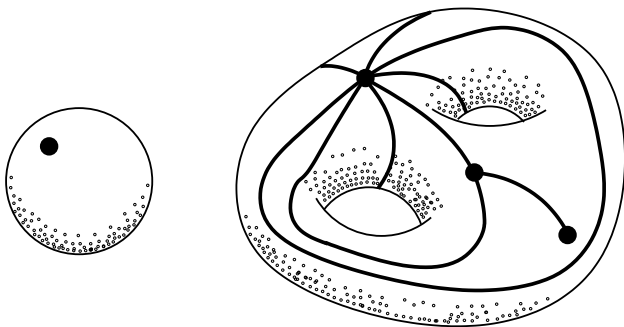


Figure 1: Two examples of topological maps on orientable surfaces: left, the easiest topological map (single vertex on a sphere, no edges and one face); right, an example of a map on an orientable surface of genus 2, familiarly called a *cow*. In this second map we can locate three vertices, six edges and one face.

¹ A regular surface is orientable if one can give an orientation on it; roughly speaking, a regular surface $S \subset \mathbf{R}^n$ is denoted as an *orientable surface* if each tangent space T_u in $u \in S$ can be connected with any other T_u with a continuous function preserving the orientation of T_u .

² A Jordan arc is an arc homeomorphic to a straight line segment.

³ If a Jordan arc contains one or more vertices inside, it splits into two or more edges.

⁴ A homeomorphism is a bijective and bicontinuous function connecting each point of Σ with each one of Σ' ; it ensures that starting object topology is kept.

⁵ The genus of a surface is, in a simple counting, the number of its holes: e.g. the three-sphere has genus 0, the torus has genus 1 and so on.

2.1.2 Rooted maps

A map is called a *rooted map* if a certain half-edge is specified among the set of the half-edges. This peculiar half-edge, becomes the *root half-edge* of the map. In short, the initial vertex is the *root* of the map and we can refer to it as the origin of the map. Here we meet the first important analogy with Feynman diagrams: there exists an “initial vertex”, which corresponds, in quantum many-body theory, to the initial point in space-time whence we start to calculate the propagator. See Figure 2 and Figure 3.

The mathematical definition of rooted map is a little more subtle. Actually, two rooted maps with the same genus, associated with two surfaces Σ and Σ' are **isomorphic** - i.e. can be regarded as a single rooted map - if the following conditions are satisfied:

- There exists a *homeomorphism* between the two surfaces Σ and Σ' ;

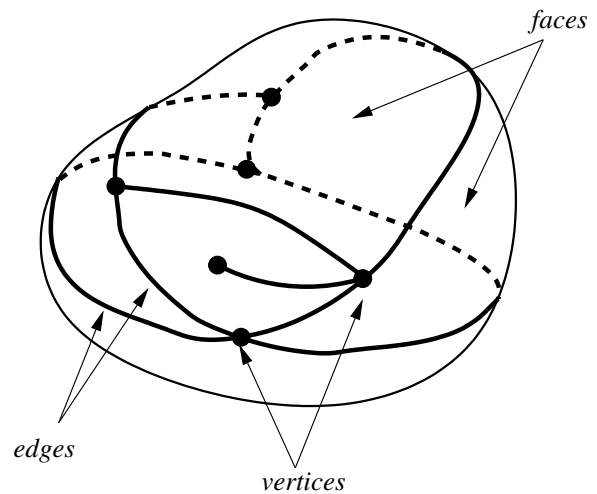


Figure 2: Example of a topological map on an orientable surface.

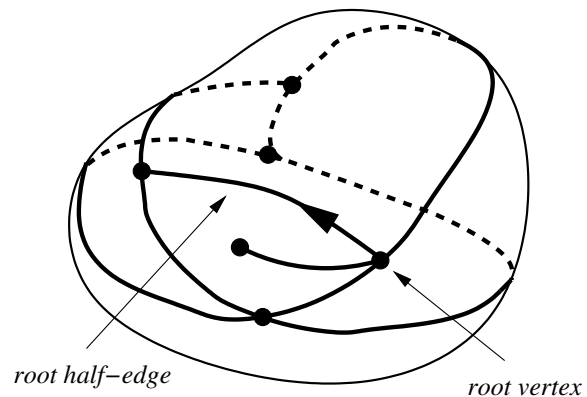


Figure 3: Example of a rooted map on an orientable surface of genus 0.

- This homeomorphism preserves the orientation of the surface;
- It maps vertices, edges, faces and the root half-edge of the first map into the homologous elements of the second one.

In fact it is the entire isomorphic class of rooted maps of the same genus that will be called a *rooted map*.

A final remark: Walsh and Lehman (among many other authors) showed also that *counting rooted maps on the projective plane or on the sphere is topologically equivalent*. Although mathematically trivial, the consequence of this remark will be extensively used in this work while *displaying* the maps in figures: for the sake of simplicity, indeed, every rooted map on the sphere will be drawn as a rooted map on the plane.

2.1.3 Euler-Poincaré invariant

One of the fundamental theorems of topology states that for any given map with V vertices, E edges and F faces - and embedded on a surface with g holes - there exists the following invariant:

$$V - E + F = 2 - 2g = \chi(g), \tag{1}$$

found as a generalization of the polyhedral formula; in Eq.(1), $\chi(g)$ is the *Euler characteristic* (or *Euler number*), sometimes also known as the Euler-Poincaré characteristic. The polyhedral formula is related to the number of polyhedron vertices V , faces F , and polyhedron edges E of a simply connected (*i.e.*, genus 0) polyhedron (or polygon).⁶ Thus the genus of maps and rooted maps can be derived from it. The only compact closed surfaces with Euler characteristic 0 are the Klein bottle and torus (Dodson and Parker [57]). We will often meet this concept in the following sections.

2.2 Enumeration of rooted maps

2.2.1 Arquès and Béraud approach

Arquès and Béraud, starting from Tutte’s results, discovered a generating function for the rooted maps series [28] namely the series which gives rise to the number of rooted

maps for a given number of vertices and edges. They proved that the generating series of rooted maps is the solution of the following Riccati’s differential equation:

$$M(y, z) = y + zM(y, z)^2 + zM(y, z) + 2z^2 \frac{\partial M(y, z)}{\partial z},$$

where y and z are respectively the number of vertices and edges. They have also shown that the generating series of rooted maps *with respect to the number of edges only* is solution of the differential equation:

$$M(z) = 1 + zM(z)^2 + zM(z) + 2z^2 \frac{\partial M(z)}{\partial z}.$$

Thanks to this relation, Arquès and Béraud found the “nice continued fraction form” for the generating series $M(y, z)$ of rooted maps with respect to the number of vertices and edges:

$$M(y, z) = \frac{y}{1 - \frac{(y+1)z}{1 - \frac{(y+2)z}{1 - \frac{(y+3)z}{1 - \dots}}}}},$$

with an important corollary: the generating series $M(y, z)$ of rooted maps with respect to vertices and edges is the solution of the following generalized Dyck’s equation:

$$M(y, z) = y + zM(y, z)M(y + 1, z).$$

By means of this corollary, the same authors found the explicit formula for the number of rooted maps with n edges:

$$M(n) = \frac{1}{2^{n+1}} \sum_{i=0}^n (-1)^i \sum_{\substack{k_1+\dots+k_{i+1}=n+1 \\ k_1, \dots, k_{i+1} \geq 0}} \prod_{j=1}^{i+1} \frac{(2k_j)!}{k_j!}.$$

The anchor conditions which appear in the second summation show that we have to sum over all the possible partitions of the integer $n + 1$ in $i + 1$ integer numbers. In the following Table 1, the first terms of this formula are shown.

Table 1: The number of rooted maps $M(n)$ on an orientable surface as a function of the number of edges n and regardless to genus, according to Arquès and Béraud [28], up to 4 edges.

n	$M(n)$
0	1
1	2
2	10
3	74
4	706

⁶ It was discovered independently by Euler and Descartes in 1752 and it is also known as the Descartes-Euler polyhedral formula. The formula also holds for some, but not all, non-convex polyhedra and it has been generalized for n -dimensional polytopes by Schläfli in 1868.

2.2.2 Walsh and Lehman approach

Walsh and Lehman [39] began their work by studying the *combinatorial equivalent of maps*: this approach allowed them to deal with the map enumeration from a combinatorial point of view (rather than a topological one). Then they gave a simple application of counting rooted maps regardless to genus. Later on, they generalized the Tutte’s recursion formula [33] for higher genus for counting *slicings* and introduced the concept of *dicing* which actually is a “contracted slicing”: in short, they considered the map obtained from slicings by contracting each band to a point. Thus a “dicing” is a map whose vertices are distinguished by labeling each vertex with a different natural number (d_i). In order to summarize this important result, let us introduce the number of dicings of a genus g surface whose vertices are of degree d_1, \dots, d_v : we define it as $C_g(d_1, \dots, d_v)$. The authors proved that the following recursion formula holds:

$$C_g(d_1, \dots, d_v) = \sum_{i=1}^{v-1} d_i C_g(d_1, \dots, d_{i-1}, d_i + d_v - 2, d_{i+1}, \dots, d_{v-1}) + \sum_{\substack{k+m=d_{v-2} \\ k \geq 0, m \geq 0}} C_{g-1}(d_1, \dots, d_{v-1}, k, m) + \sum_{\substack{D_1 \cup D_2 = d_1 + \dots + d_{v-1} \\ D_1 \cap D_2 = \emptyset}} \sum_{\substack{h+f=g \\ k+m=d_{v-2} \\ k \geq 0, m \geq 0}} C_h(D_1, k) C_f(D_2, m). \tag{2}$$

This formula reduces to the Tutte’s recursion formula [33] when $g = 0$. For further details, such as the explicit combinatorial meaning of dicings or the proof of uniqueness of the solution of the Walsh and Lehman’s recursion formula, see [39]. By means of (2), they computed the number of dicings given the degree of each vertex and the genus. In particular, Walsh and Lehman extracted an explicit formula for maps with one face. Finally, they obtained a relation between the number of dicings and the number of rooted maps. This relation allows to calculate the number of rooted maps with respect to the genus, the number of vertices and the number of edges. In other words, they obtained the following relation: if we denote with

$C_g(d_1, \dots, d_v)$ the number of dicings and an explicit expression is known for it, the number of rooted maps of genus g , with v vertices and e edges is:

$$\frac{2e}{v!} \sum_{d_1+d_2+\dots+d_v=2e} \frac{C_g(d_1, d_2, \dots, d_v)}{\prod_{i=1}^v d_i}.$$

Summing over all the descending sequences (d_1, \dots, d_v) which add to $2e$ gives the number of rooted maps of genus g with e edges and v vertices. In this way they were able to fill the Table I of Ref. [39]. An extract of this result is shown in Table 2. Interestingly, if we sum the number of maps with n -edges (*i.e.* independently of the genus g), we obtain the sequence 1, 2, 10, 74, 706, ... *i.e.* the number of rooted maps as a function of the number of edges and regardless to genus, as found by Arquès and Béraud [28] (see

Table 2: The number of rooted maps with e edges and v vertices by genus g up to 4 edges. From [39], p. 215. The last (supplementary) column corresponds to Table 1 and contains the first terms of the Arquès-Walsh sequence: 1, 2, 10, 74, 706, ...

e	v	$g = 0$	$g = 1$	$g = 2$	\sum per edges
0	1	1			1
1	1	1			2
	2	1			
2	1	2	1		10
	2	5			
	3	2			
3	1	5	10		74
	2	22	10		
	3	22			
	4	5			
4	1	14	70	21	706
	2	93	167		
	3	164	70		
	4	93			
	5	14			

7 The problem actually is to find an explicit expression for the term $C_g(d_1, d_2, \dots, d_v)$. Walsh and Lehman for instance found an explicit form for the rooted maps with *one* face, where $d_1 + \dots + d_v = 4g + 2v - 2$, which leads to the very interesting formula:

$$M(n, v, g)_{\text{one face}} = \frac{(2v + 4g - 2)!}{2^{2g} v! (v + 2g - 1)!} \sum_{\substack{i_1 + \dots + i_v = g \\ i_1, \dots, i_v \geq 0}} \prod_{j=1}^v \frac{1}{1 + 2i_j}.$$

This is the number of rooted maps of genus g with one face, v vertices and $v + 2g - 1$ edges and, by duality between vertices and faces, it is also the number of rooted maps of genus g with one vertex, v faces and $v + 2g - 1$ edges. Compare this expression with the $M(n)$ of the next section.

Table 1). We will refer to this sequence as to the **Arquès-Walsh sequence**.

3 Feynman diagrams and rooted maps

As anticipated in the Introduction, the main purpose of the present work lies in the connection between counting rooted maps and enumerating Feynman diagrams in the perturbative series which expresses the single particle Green's function (or propagator) within the non-relativistic many-body theory of a system of fermions (particles with half-integer spin).

Without any pretense of completeness, we recall here only the starting point, key formulas and definitions, which lead to the perturbative expression one can represent in terms of Feynman diagrams. The reader is addressed, e.g., to the Fetter and Walecka textbook [58] or the more recent ones by Dickhoff and Van Neck [59] and by Stefanucci and Van Leeuwen [60] for a comprehensive derivation of the pertinent formulas.

The physical system is described by an Hamiltonian operator

$$\hat{H} = \hat{H}_0 + \hat{H}_1$$

where \hat{H}_0 corresponds to a non-interacting (solvable) system, while \hat{H}_1 contains the (two-body) interaction between the constituents of the system.

The single-particle Green's function is then defined by

$$i\mathcal{G}_{\alpha\beta}(x, y) = \frac{\langle \Psi_0 | T[\hat{\Psi}_{H_\alpha}(x)\hat{\Psi}_{H_\beta}^\dagger(y)] | \Psi_0 \rangle}{\langle \Psi_0 | \Psi_0 \rangle} \quad (3)$$

where $|\Psi_0\rangle$ is the exact ground state of the system, $\hat{\Psi}_{H_\alpha}$ ($\hat{\Psi}_{H_\beta}^\dagger$) are field operators in Heisenberg representation, destroying (creating) a particle in a specific space-time point with the appropriate spin projection. T is the time-ordered product, forcing the operator with the latest time to be placed on the left. The quantity in Eq.(3) also represents the propagation of the interacting particle from point $x \equiv (\mathbf{x}, t_x)$ to $y \equiv (\mathbf{y}, t_y)$ (or vice versa).

Perturbation theory leads then, with the help of a few celebrated quantum fields theorems, to the expression:

$$i\mathcal{G}_{\alpha\beta}(x, y) = \sum_{m=0}^{\infty} \left(-\frac{i}{\hbar}\right)^m \frac{1}{m!} \int_{-\infty}^{+\infty} dt_1 \cdots \int_{-\infty}^{+\infty} dt_m \quad (4)$$

$$\langle \Phi_0 | T[\hat{H}_1(t_1) \cdots \hat{H}_1(t_m) \hat{\Psi}_\alpha(x) \hat{\Psi}_\beta^\dagger(y)] | \Phi_0 \rangle_{\text{connected}}$$

where m is the order of the perturbative term and all operators are in Interaction representation, $|\Phi_0\rangle$ being now

the ground state of the non-interacting system. Notably it can be shown that the series extends only to the connected terms, namely those terms where the interaction Hamiltonians are connected to the “fixed” external points x, y , or equivalently to the fermion propagator running from y to x . The terms of Eq.(4) and their enumeration can be put into a one to one correspondence with Feynman diagrams, according to the rules explained in the Appendix.

A detailed enumeration of Feynman diagrams according to their physical properties (and as a function of the perturbative order) is presented in the work of Cvitanović, Lautrup and Pearson [27]. In particular, Table I contains the reckoning of several subtypes of QED diagrams. The first two columns show the effect of the Furry's theorem which cancels a large number of diagrams in QED. Conversely, in many-body theory, all the diagrams which appear in the first column (“Exact electron propagators without Furry's theorem”) can contribute to the total amplitude⁸. The reason why in many-body theory the Furry's theorem is not active lies in the different nature of the *vacuum* in the two approaches: the Dirac sea with an infinite number of negative energy states in QED and the (unperturbed) ground state of N particles in many-body theory (Fermi sea). Clearly vacuum loops diverge in QED and are removed by standard renormalization procedures. Since these divergences do not occur in many-body theory, the number of Feynman diagrams (as a function of the perturbative order for the exact electron propagator) without taking into account Furry's theorem is

$$1, 2, 10, 74, 706 \dots$$

Remarkably, **it corresponds to the Arquès-Walsh sequence**, i.e. to the number of rooted maps regardless to genus and vertices as a function of the number of edges. The numerical correspondence is quite striking and it is suggestive that between this two objects, the physical ones (Feynman diagrams) on the one side and the mathematical ones (rooted maps) on the other side, there exists a topological connection. Our aim is then to explore this topological equivalence. This goes beyond a simple *counting* of these objects (which corresponds to compare the Arquès formulas on pages 6-10 of [28] with the ones of Cvitanović [27] on page 1943). The purpose is rather to discover *how* a Feynman diagram is related to a rooted map.

⁸ In this Table, Cvitanović, Lautrup and Pearson use a different notation: they refer to the perturbative order of a Feynman diagram as to the number of interaction vertices: this is indeed customary in QED, where the fundamental interaction Lagrangian refers to the electron-photon coupling. In this framework the exchange of a photon between two electrons is viewed as a second-order term.

It is in fact the *topology* of these objects which entails their *physical* content (while an exact match between these formulas is rather of a mathematical interest).

3.1 Connection between diagrams and maps

On the *physical* side, the starting point is the book Ref. [58–60], where the Feynman diagrams (at first and second-order) are explicitly drawn⁹. On the *mathematical* side, the starting point is the work of Tutte [34], where the (planar) rooted maps (up to 2 edges) are also explicitly drawn¹⁰. Figure 4 shows the easiest (non-trivial) examples of Feynman diagrams (left) at first-order of perturbation: diagram *a* (also known as “shell”) contains no loops while diagram *b* (also known as “tadpole”) contains one loop. Figure 4 (right) shows also the first 2 non-trivial rooted maps with one edge and one vertex (map *c*) and two vertices (map *d*). We will use the two diagrams and the two maps to illustrate a graphical, step-by-step association (which will be indicated as the *quotient procedure*) - for the first-order diagrams (or for the rooted map with one edge) - between these two kinds of objects.

3.1.1 Quotient procedure (first-order)

The following steps illustrate an intuitive way to associate a rooted map to a given Feynman diagram (at first order). They do not represent a rigorous proof of the association,

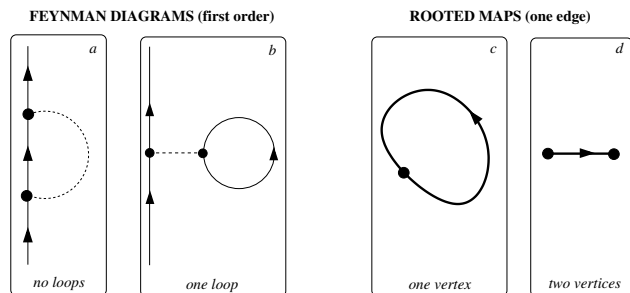


Figure 4: The easiest (non-trivial) Feynman diagrams and (non-trivial) rooted maps as they appear in Refs. [58] and [34], respectively. Interaction lines are represented with dashed lines, propagation lines with solid ones.

⁹ The work of Cvitanović [27] will help us to enumerate and distinguish the physics properties of Feynman diagrams at any order.

¹⁰ The work of Walsh and Lehman [39] (summarized in Table 2) will help us with the detailed enumeration of the rooted maps according to their number of vertices, edges and the genus of the embedding surface.

but they will help us to investigate the topological equivalence between diagrams and maps. As a preliminary remark, we recall that for each Feynman diagram, an “initial” point and a “final” point can always be defined without any ambiguity: these points represent the initial and final positions in spacetime between which we evaluate the Green’s function¹¹.

- Starting from a Feynman diagram (step **A** of Figure 5), we connect its initial (*i*) and final (*f*) points, obtaining a new object: the **closed graph** (step **B**). The obtained (oriented) arc will be defined as the *rooted arc*¹². All the propagation-line arrows will be left out, except for the one on the rooted arc.
- Starting from the point $i = f$ in the closed graph, we travel the rooted arc (e.g. counterclockwise) till the first interaction line and we shift the rooted arc arrow on it. Then, all the interaction lines will be drawn as solid lines and all the propagation lines will be drawn as dotted lines, obtaining the **quotient graph** (step **C**). The (unique) solid line carrying the arrow will be referred as to the *rooted edge*.
- All the dotted lines in the quotient graph are collapsed to a unique vertex each. The result is a rooted map (step **D**).

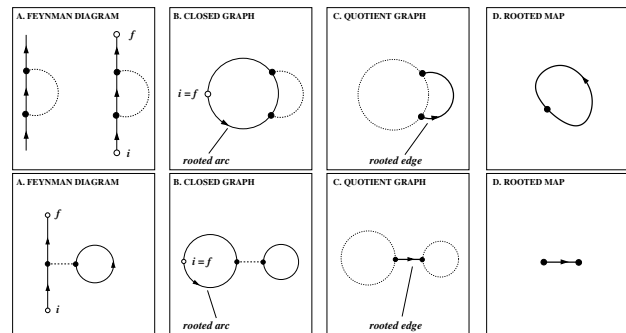


Figure 5: (Top) Association of the first-order Feynman diagram *a* to the rooted map *c* of Figure 4 by means of the *quotient procedure*. (Bottom) Association of the first-order Feynman diagram *b* to the rooted map *d* of Figure 4. The “initial” (*i*) and “final” (*f*) points are shown.

¹¹ These points are easily distinguished in the diagram, since they are the only vertices of a propagation line that are not connected to an interaction line.

¹² The rooted arc can be obtained either connecting *i* and *f* lefthandwise or righthandwise (so that the rooted arc results oriented counterclockwise or clockwise, respectively). This choice will not affect the results, provided that we apply the same rule for all the diagrams. Here we will use the first one.

3.1.2 Quotient procedure (second and higher order)

If we try to apply the previous steps to the second-order diagrams in Ref. [58] (see Figure 6 and 7), we have no difficulties till the diagram number 10. The peculiarity of such a diagram can be seen under two perspectives. First, its quotient graph contains a **crossing** (such a characteristic never occurred in all the other graph). Second, we already know that there should be *nine* (planar) rooted maps with two edges (these are the maps drawn by Tutte): but we also know (see again Table 2) that one *and only one* rooted map with two edges should be embedded **on the torus**. This means that another step must be added to the quotient procedure: the quotient graph should be embedded on an orientable surface *with the minimum number of holes as it is needed to remove all the crossings* (step E). We show in

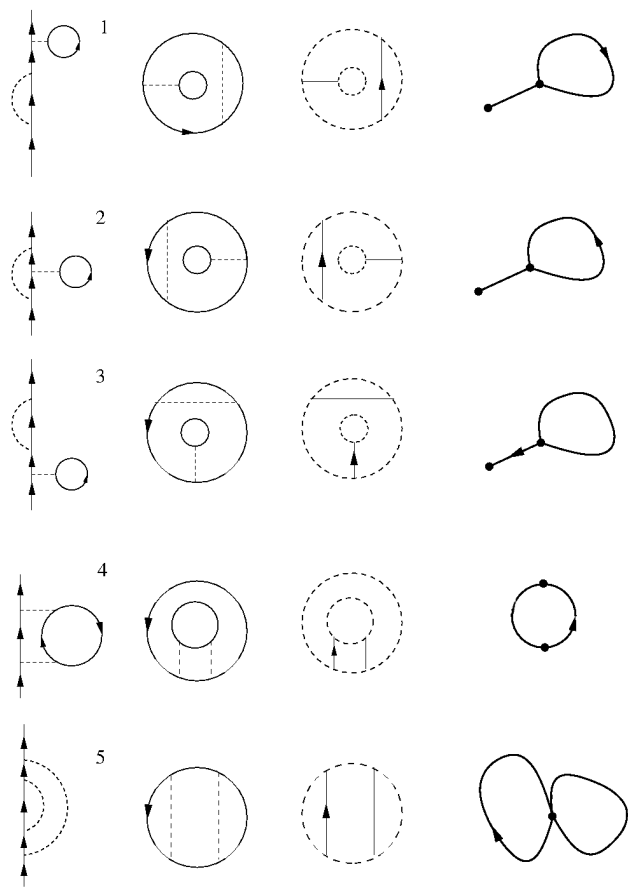


Figure 6: Association of the second-order Feynman diagrams (as they appear in [58]) with the two-edges rooted maps (on the sphere) as they appear in [34] by means of the *quotient procedure*. In the first column, the Feynman diagrams at second perturbative order (*i.e.* with 2 interaction lines) are shown. In the second and third columns the related closed graphs (with their rooted arc) and quotient graphs (with their rooted edge) are shown. The last column contains the resulting rooted maps. The list continues in Figure 7.

Figures 8 and 9 some intriguing examples of order higher than two.

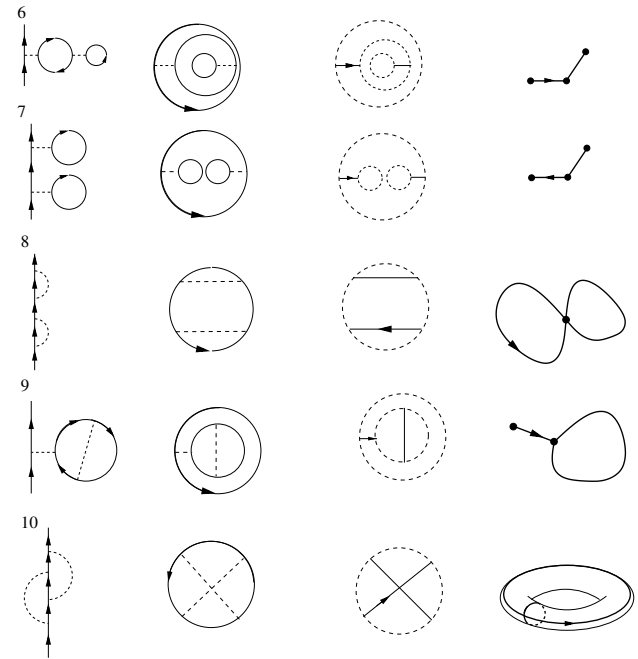


Figure 7: Continues from Figure 6. Notably, the rooted map related to the Feynman diagram n.10 is embedded on a torus.

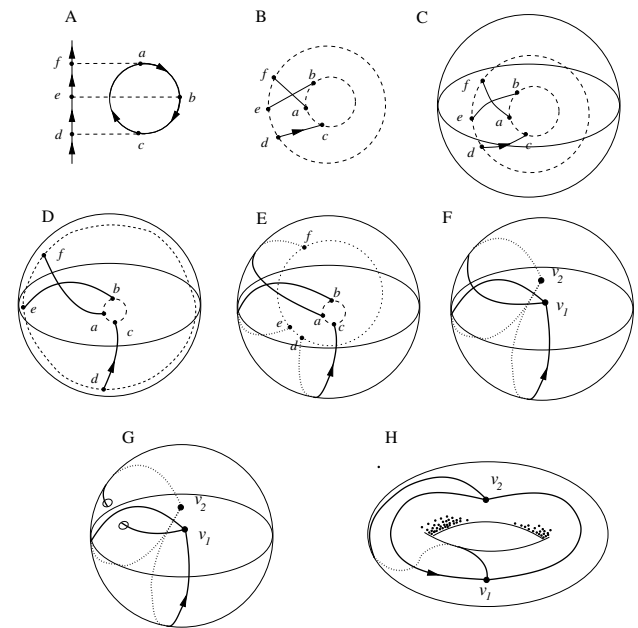


Figure 8: The quotient procedure applied to a third-order Feynman diagram. Once we have embedded its quotient graph on an orientable surface (for example a sphere, frame C), we collapse the dashed lines into vertices (here v_1 and v_2), while maintaining the relative positions of the interaction-line extremes $a, b, c \dots$ on their dashed lines (see pictures D-E-F). In order to remove the crossings between the resulting edges, we add a hole into the surface.

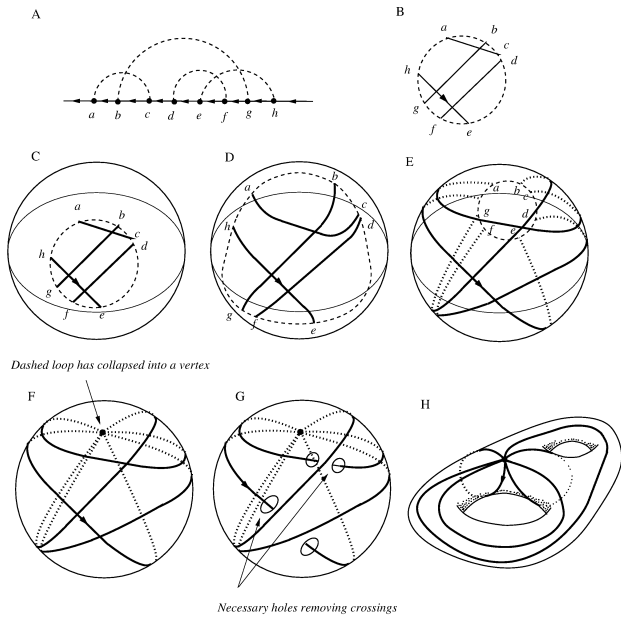


Figure 9: The quotient procedure applied to a fourth-order Feynman diagram. In order to remove the crossings in the quotient graph, one hole is not enough. The associated rooted map results actually embedded on the cow.

3.1.3 Quotient procedure (full third-order)

Let us consider the third-order diagrams derived in the Appendix. We have first applied the quotient procedure to all the shell diagrams shown in Figure 8 the remaining third-order diagrams can be found in the Appendix, where a simple method to build Feynman diagrams at any order is also presented. It was needed to recover the exact shape of each of the 74 diagrams at third-order. Actually, a publication where these 74 Feynman diagrams are explicitly drawn is not available, at variance with the second-order diagrams, which can be easily found in the literature. We can immediately observe that there are 10 diagrams which contain unremovable crossings between the interaction lines (we are talking about number 2, 3, 6, 7, 8, 9, 10, 11, 12, 14) and 5 diagrams without crossings (number 1, 4, 5, 13 and 15). Thanks to Table 2, we could predict that there could be only *five* diagrams on the sphere. If we apply the quotient procedure to the diagrams of Figures 10, 11 and 12, we find indeed five and only five rooted maps on the sphere (diagrams number 1, 2, 3, 13 and 15 in the above mentioned figures). Let us analyze the number of vertices of this maps: we find that all of them have *one* vertex. But if we check our Table 2, we discover that on the sphere *there are just five rooted maps with 3 edges and only one vertex*. This also ensures the validity of the the quotient procedure and

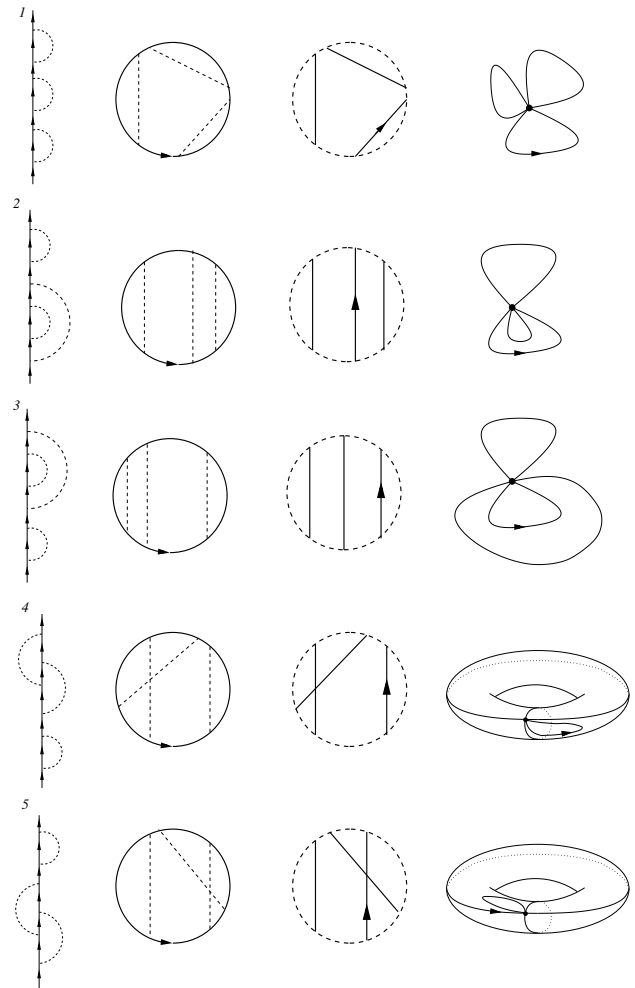


Figure 10: Closed and quotient graphs of “shells” Feynman diagrams and their related rooted maps, obtained by means of the quotient procedure. Feynman diagrams which are not embedded on a sphere are related to a map on the torus.

hence the validity of the one-to-one correspondence with rooted maps on the sphere at this stage.¹³

We show all the quotient graphs of the remaining third-order Feynman diagrams in Figures 13, 14, 15, 16, 17, 18, 19, 20, 21, 22, 23.

3.1.4 Remarks

Comparing the Tutte’s rooted maps and the list of first, second and third-order Feynman diagrams we can easily con-

¹³ Notice that - if the quotient procedure is right - *there could not be* other maps with 3 edges, one vertex and genus 1, related to the five Feynman diagrams. In fact, if we check the Walsh work [39] on page 215, we do not find any other map with these features.

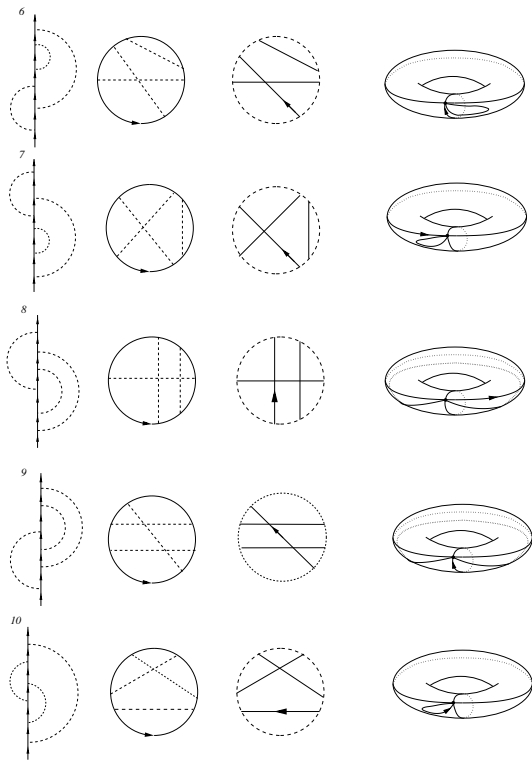


Figure 11: Closed and quotient graphs of “shells” Feynman diagrams and their related rooted maps (*continued*).

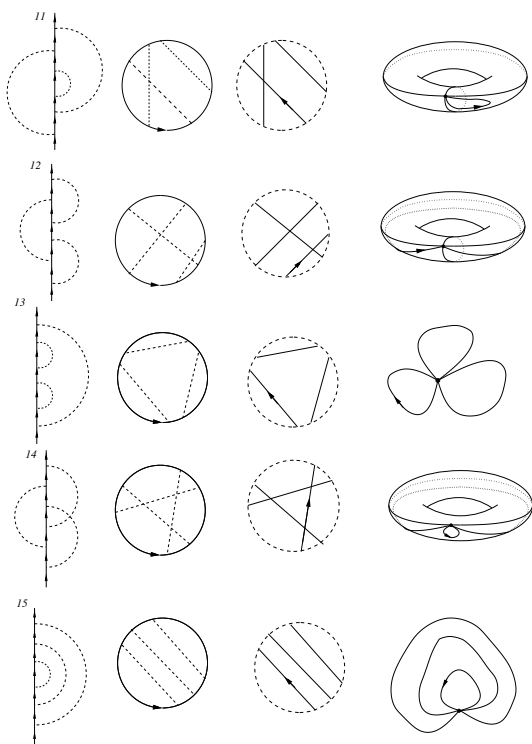


Figure 12: Closed and quotient graphs of “shells” Feynman diagrams and their related rooted maps (*continued*).

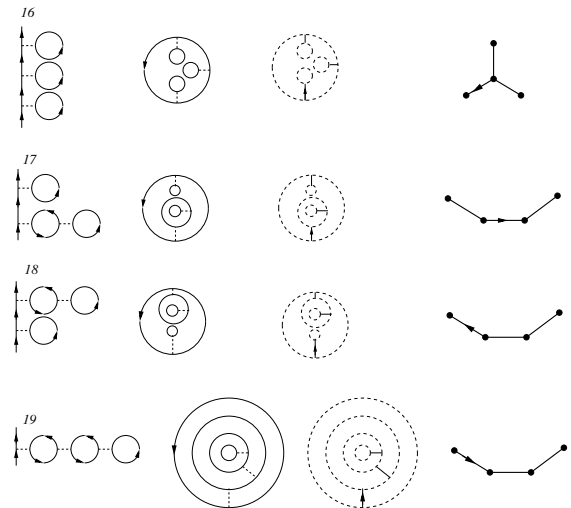


Figure 13: Closed and quotient graphs of other third-order diagrams and their related rooted maps.

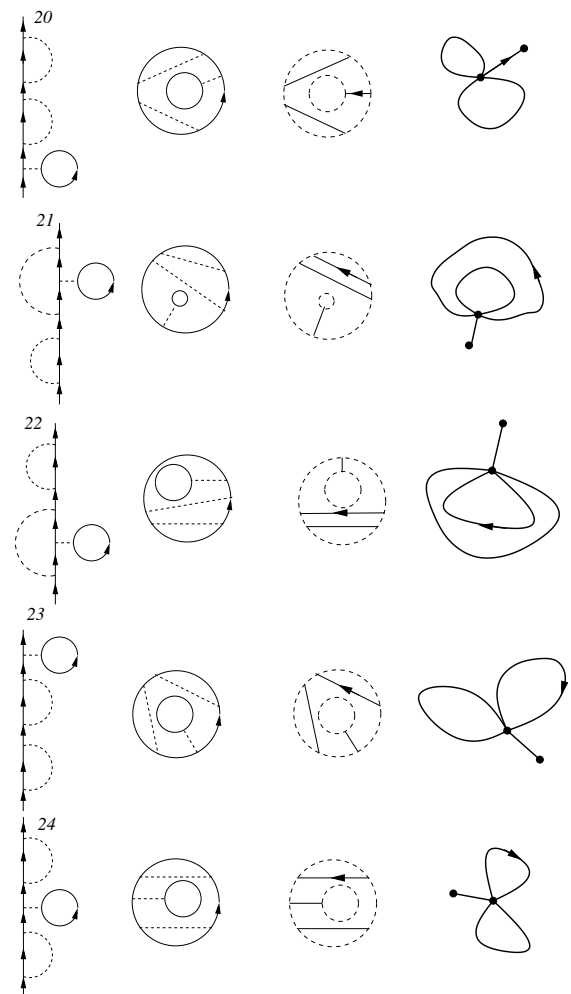


Figure 14: Closed and quotient graphs of other third-order diagrams and their related rooted maps.

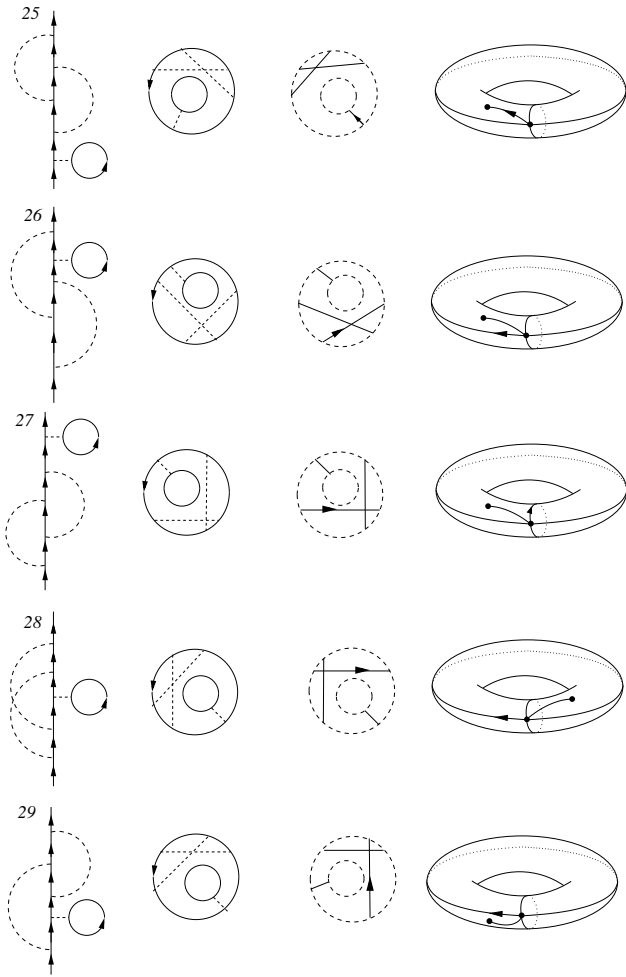


Figure 15: Closed and quotient graphs of other third-order diagrams and their related rooted maps.

clude that every Feynman diagram of the n -th order with l loops - and without crossing either between any interaction lines or between interaction and propagation lines - is related to one (and only one) rooted map embedded in a sphere-like surface with n edges and $l+1$ vertices. Through the quotient procedure, in fact, an additional loop is created (the one which contains the root edge) but all the propagation lines, after the shrinking procedure, become a point. For this reason the l loops become $l + 1$ vertices (which are actually points). Moreover, through the same procedure, the interaction lines of the original Feynman diagram are not modified so that they directly become the edges of the map. We can check the validity of this procedure by verifying that we have just obtained:

- 2 rooted maps on the sphere starting from the 2 Feynman diagrams at first order; among these 1-edge maps, we have obtained: 1 rooted map with 1 vertex and one map with 2 vertices.

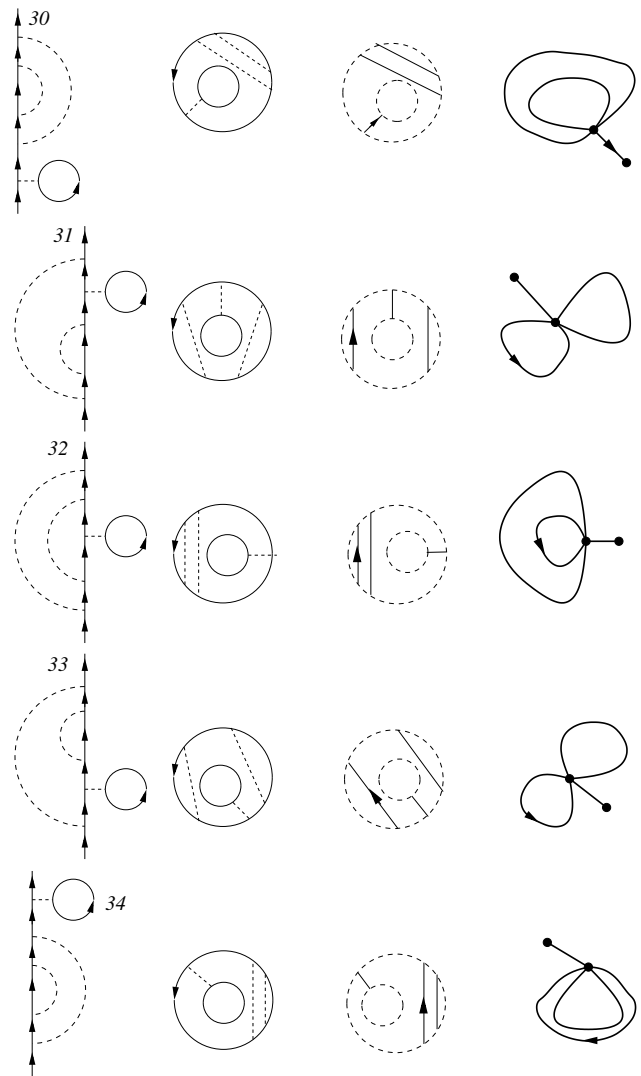


Figure 16: Closed and quotient graphs of other third-order diagrams and their related rooted maps.

- 9 rooted maps on the sphere starting from the 10 Feynman diagrams at second-order; among these 2-edges maps there are 2 maps with one vertex, 5 maps with 2 vertices and 2 maps with 3 vertices.
- 54 rooted maps with 3 edges on the sphere starting from the 74 Feynman diagrams at third-order. 5 of them have just 5 vertices, 22 of them have 2 vertices and other 22 have 3 vertices; finally we have obtained, among this class of maps with 3 edges, 5 maps with 4 vertices.

This is a remarkable result because it is in perfect agreement with the works by Bender and Canfield and with the ones by Walsh and Lehman (see Table 2).

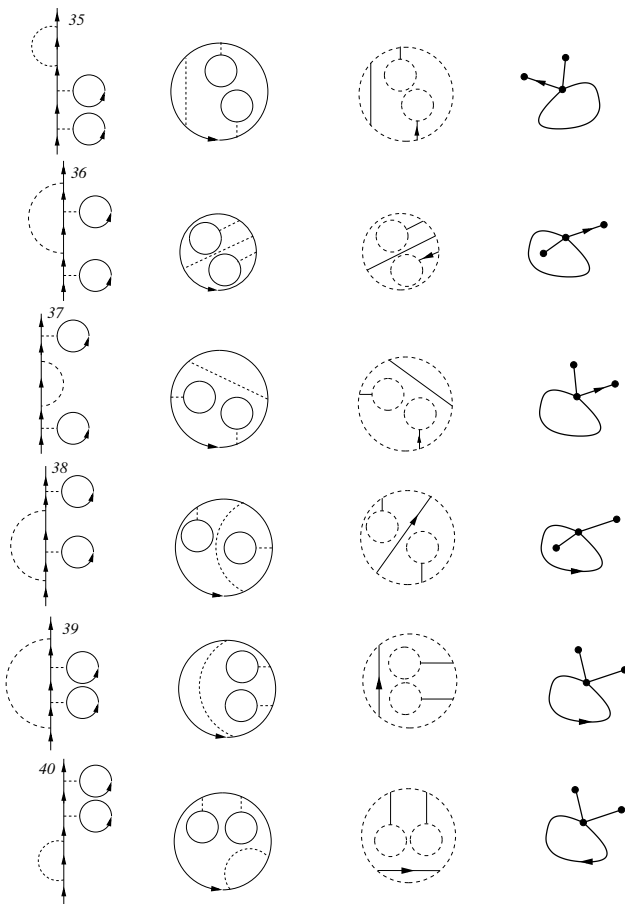


Figure 17: Closed and quotient graphs of other third-order diagrams and their related rooted maps.

3.2 The genus of a Feynman diagram

Finding the embedding of a graph was shown to be a NP-complete problem (see for instance Carsten [61]). However, the existence of a precise association between Feynman diagrams and maps (based on the quotient procedure) strongly suggests that Feynman diagrams and rooted maps **are isomorphic mathematical object**. Thus, it becomes natural to define *the genus of a Feynman diagram* as the genus of the related rooted map, *i.e.* the genus of the orientable surface in which the related rooted map is embedded. However, this definition is quite different from the one given in the work by J. S. Kang [62], where the genus (G) of the Feynman diagram is defined as

$$V - P + I = 2 - 2G. \quad (5)$$

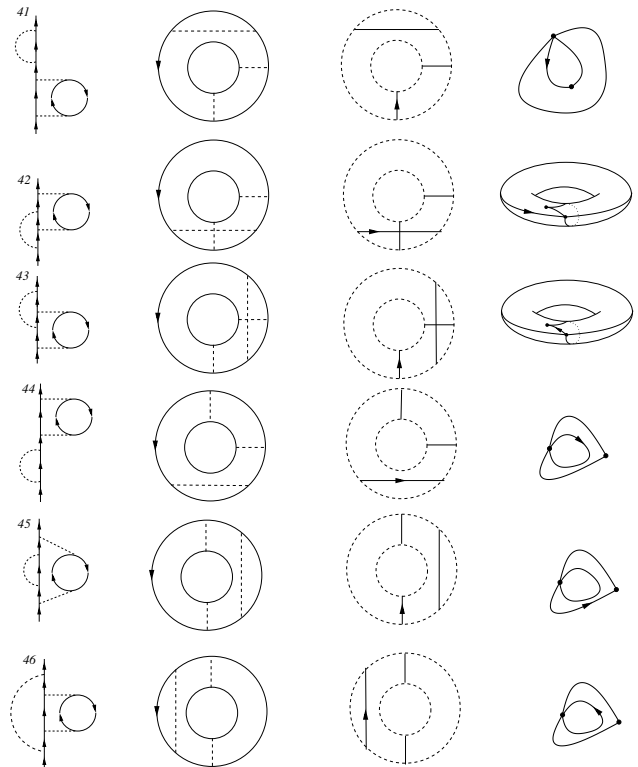


Figure 18: Closed and quotient graphs of other third-order diagrams and their related rooted maps.

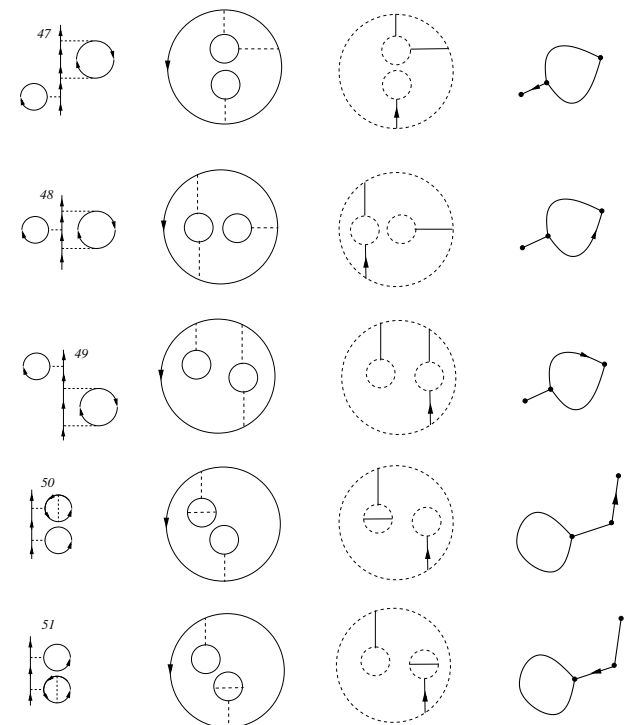


Figure 19: Closed and quotient graphs of other third-order diagrams and their related rooted maps.

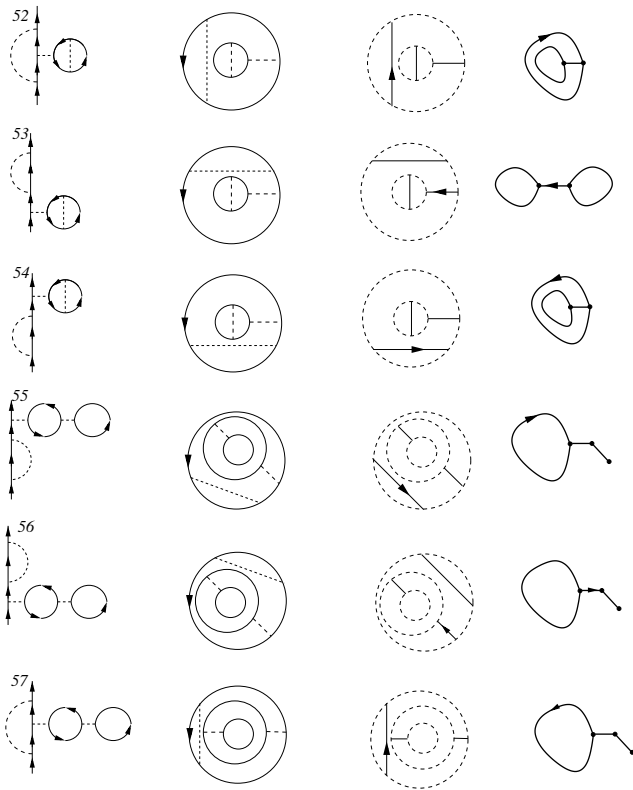


Figure 20: Closed and quotient graphs of other third-order diagrams and their related rooted maps.

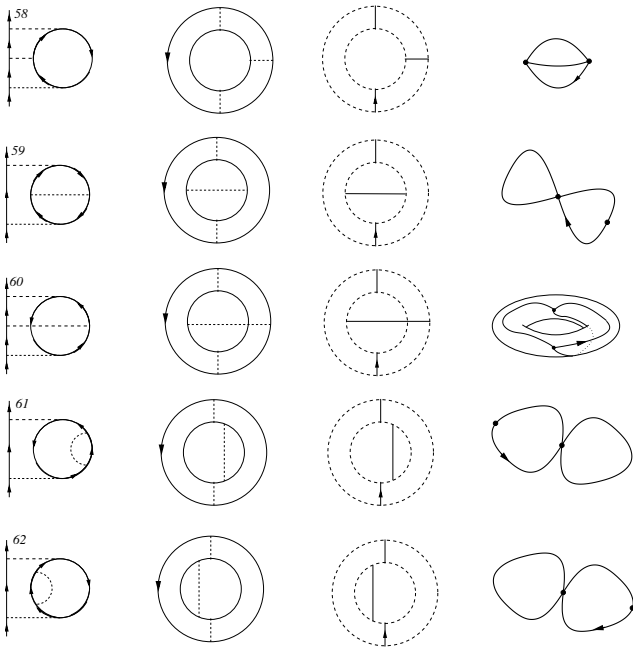


Figure 21: Closed and quotient graphs of other third-order diagrams and their related rooted maps.

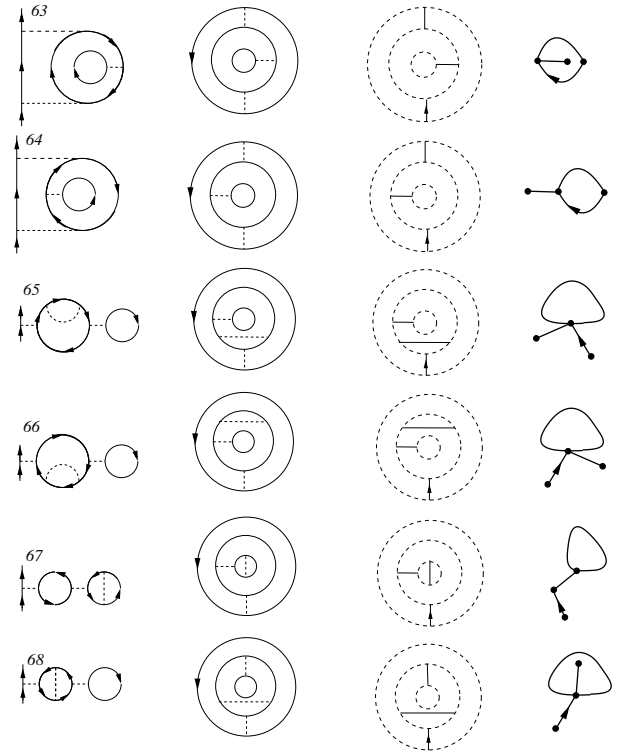


Figure 22: Closed and quotient graphs of other third-order diagrams and their related rooted maps.

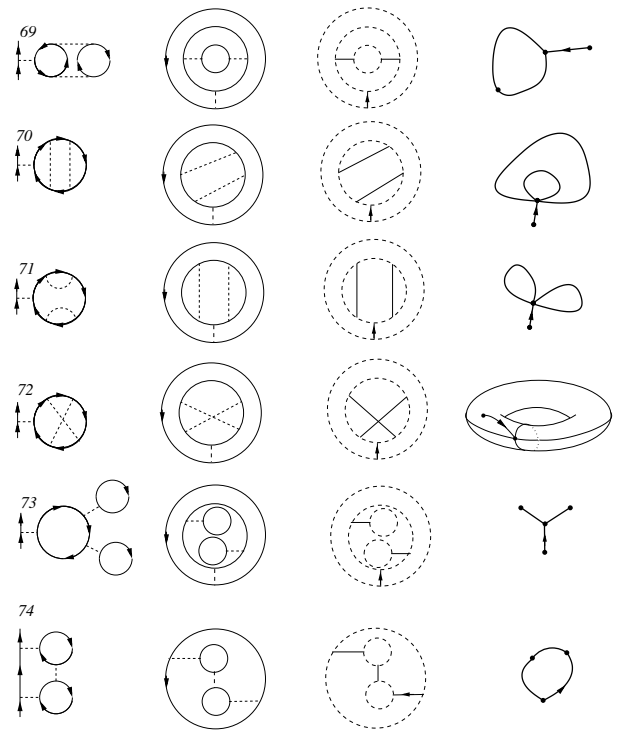


Figure 23: Closed and quotient graphs of other third-order diagrams and their related rooted maps.

Here V is the number of vertices, P the number of propagators and I the number of the closed loops. This definition is followed by many authors like Gross, Mikhailov and Roiban [63], Nayak [64] or Schwarz [65]. We propose, instead, a definition which start from the well known Euler characteristic of a rooted map:

$$v - e + f = 2 - 2g, \tag{6}$$

where v is the number of the vertices of the map, e the number of its edges and f the number of its faces. Then we substitute the number of vertices with $v = l + 1$:

$$(l + 1) - e + f = 2 - 2g, \tag{7}$$

where l is the number of loops in the associated Feynman diagram, f and g are respectively the number of faces and the number of holes of the related rooted map (namely the genus of the orientable surface in proper sense). Thus the genus of Feynman diagrams provided by Eq.(7) is similar to the one of formula (5) *only* in the sense that both equations derive from the Euler-Poincaré formula. But the numbers G and g associated to the same diagram are usually different and only accidentally coincide, as reported in Table 3.

Table 3: Comparison between the Kang’s definition of the genus G of a Feynman diagram Eq.(5) and the genus g calculated by our definition Eq.(7), with regard to the Feynman diagrams (n.1, n.2, ...) represented in Figure 6 and Figure 7.

diagrams	vertices-propagators+loops= $2 - 2G$
n.1	$4 - 5 + 1 = 2 - 2G \rightarrow G = 1$
n.2	$4 - 5 + 1 = 2 - 2G \rightarrow G = 1$
n.3	$4 - 5 + 1 = 2 - 2G \rightarrow G = 1$
n.4	$4 - 5 + 1 = 2 - 2G \rightarrow G = 1$
n.5	$4 - 5 + 0 = 2 - 2G \rightarrow G = \frac{3}{2}$
n.6	$4 - 5 + 2 = 2 - 2G \rightarrow G = \frac{1}{2}$
n.10	$4 - 5 + 0 = 2 - 2G \rightarrow G = \frac{3}{2}$
diagrams	(loops+1)-edges+faces= $2 - 2g$
n.1	$2 - 2 + 2 = 2 - 2g \rightarrow g = 0$
n.2	$2 - 2 + 2 = 2 - 2g \rightarrow g = 0$
n.3	$2 - 2 + 2 = 2 - 2g \rightarrow g = 0$
n.4	$2 - 2 + 2 = 2 - 2g \rightarrow g = 0$
n.5	$1 - 2 + 3 = 2 - 2g \rightarrow g = 0$
n.6	$3 - 2 + 1 = 2 - 2g \rightarrow g = 0$
n.10	$1 - 2 + 1 = 2 - 2g \rightarrow g = 1$

4 Summary and conclusions

In this work we have shown, up to third-order in perturbation theory, the perfect agreement between the number of Feynman diagrams as a function of the perturbative order and the number of rooted maps on orientable surfaces as a function of the number of edges (and regardless to genus and to the number of vertices on the map).

This result has been obtained by establishing a graphical correspondence between Feynman diagrams and rooted maps on the sphere and on oriented surfaces of higher genus. The quotient procedure presented here contains definite and unambiguous rules which allow to obtain the rooted map corresponding to a generic Feynman diagram. In this connection it is worth pointing out that in the Appendix we define a simple but effective procedure for building Feynman diagrams at any order in perturbation theory from a purely graphical point of view.

A new definition of the *genus of a Feynman diagram* has also been given: the genus of a Feynman diagram is the number of holes of the surface in which the corresponding rooted map is embedded. Hence one might conjecture that Feynman diagrams and rooted maps are the same topological object. The information about the physics is totally embodied in the number of vertices, edges, faces and holes of the embedding surface and their mutual relations.

It should be stressed that in this work we have considered Feynman diagrams entering into the perturbative expansion of the single-particle propagator within a many-body context. Other classes of diagrams, for example in the two-body propagator or the polarization propagator, as well as in the diagrammatic representation of the perturbative contributions to the ground/excited state energy of the system (Goldstone diagrams) are crucial for the correct determination of the observables. Starting from the results of the present work it should be possible to calculate some specific class of diagrams such as “ladder or skeleton”, “RPA”, and “irreducible” diagrams by means of rooted maps theory. In the present work we concentrate on the single particle propagator: here the most interesting development is the internal resummation of proper (non-separable) self-energy diagrams, which leads to the Dyson (integral) equation. The perturbative expansion is thus manipulated in such a way to include some class of diagrams up to infinite order. In particular it could be interesting a comparative approach to “non-separable maps”, but this goes well beyond the scope of this paper.

References

- [1] Floer A., The unregularized gradient flow of the symplectic action, *Comm. Pure Appl. Math.*, 1988, 41(6), 775-813.
- [2] Floer A., Witten's complex and infinite-dimensional Morse theory. *J. Diff. Geom.*, 1989, 30, 202-221.
- [3] Floer A., An instanton-invariant for 3-manifolds, *Comm. Math. Phys.*, 1988, 118, 215-240.
- [4] Fukaya K., Morse homotopy and its quantization, In: W. H. Kazez (ed.) *Geometric Topology*, Georgia International Topology Conference (August 2-13, 1993, Athens, Georgia, USA), *Ams/Ip Studies in Advanced Mathematics*, Amer. Math. Soc., 1996, 409-441.
- [5] Fukaya K., Morse homotopy and Chern-Simons perturbation theory, *Comm. Math. Phys.*, 1996, 181, 37-90.
- [6] Fukaya K., Oh Y.-G., Ohta H., Ono K., Antisymplectic involution and Floer cohomology, *Geom. & Topol.*, 2017, 21, 1-106.
- [7] Fukaya K., Oh Y.-G., Ohta H., Ono K., Lagrangian Floer theory on compact toric manifolds I, *Duke Math. J.*, 2010 151, 23-174.
- [8] Goupi A., Schaeffer G., Factoring N-Cycles and Counting Maps of Given Genus, *Europ. J. Combin.*, 1998, 19(7), 819-834.
- [9] Schaeffer G., Jacquard B., A Bijective Census of Nonseparable Planar Maps, *Journal of Combinatorial Theory, Series A*, 1998, 83(1), 1-20.
- [10] Bousquet-Melou M., Schaeffer G., Enumeration of Planar Constellations, *Adv. Appl. Math.*, 2000, 24, 337-368.
- [11] Poulalhon D., Schaeffer G., A bijection for triangulations of a polygon with interior points and multiple edges, *Theoret. Comp. Sci.*, 2003, 307(2), 385-401.
- [12] Bonichon N., Gavoille C., Hanusse N., Poulalhon, D, Schaeffer, G., Planar Graphs, via Well-Orderly Maps and Trees, *Graphs and Combinatorics*, 2006, 22(2), 185-202.
- [13] Fusy E., Poulalhon D., Schaeffer G., Bijective counting of plane bipolar orientations and Schnyder woods, *European J. Combin.*, 2009, 30(7), 1646-1658.
- [14] Atiyah M., New invariants of 3- and 4-dimensional manifolds, In: Wells Jr R.O. (ed.), *Proceedings of Symposia in Pure Mathematics*, 1988, 48, 285-299. Paper presented at the mathematical heritage of Hermann Weyl, (12-16 May, 1987, Durham, NC), American Mathematical Society (Providence, RI).
- [15] Witten E., Supersymmetry and Morse theory, *J. Diff. Geom.*, 1982, 17, 661-692.
- [16] Cachazo F., Svrcek P., Witten E., MHV vertices and tree amplitudes in gauge theory, *J. High Energy Phys.*, 2004, 09, 006.
- [17] Hooft G., Dimensional Reduction in Quantum Gravity, 1993, arXiv:gr-qc/9310026v2
- [18] Ivanyos G., Klauck H., Lee T., Santha M., de Wolf R., New bounds on the classical and quantum communication complexity of some graph properties, 2012, arXiv:1204.4596v1
- [19] Di Francesco P., Ginsparg P.H., Zinn-Justin J., 2D Gravity and Random Matrices, *Phys. Rep.*, 1995, 254, 1.
- [20] Rosicky P.J., Karplus M., The enumeration of Goldstone diagrams in many-body perturbation theory, *J. Chem. Phys.*, 1976, 64, 1596.
- [21] Kuchinskii E.Z., Sadovskii M. V., Combinatorial analysis of Feynman diagrams in problems with a Gaussian random field. *J. Experim. Theoret. Phys.*, 1998, 86(2), 367.
- [22] Kleinert H., Pelster A., Kasteing B., Bachmann M., Recursive graphical construction of Feynman diagrams and their multiplicities in ϕ^4 and ϕ^2 A theory, *Phys. Rev. E*, 2000, 62, 1537-1559.
- [23] Riddel Jr R.J., The number of Feynman diagrams, *Phys. Rev.*, 1953, 91, 1243.
- [24] Brouder Ch., Runge-Kutta methods and renormalization, *Europ. Phys. J. C*, 2000, 12(3), 521-534.
- [25] Brouder Ch., On the trees of quantum fields, *Europ. Phys. J. C*, 2000, C12(3), 535-549.
- [26] Brouder Ch., Frabetti A., Renormalization of QED with planar binary trees, *Europ. Phys. J. C*, 2001, 19(4), 715-741.
- [27] Cvitanović P., Lautrup B., Pearson R.B., Number and weights of Feynman diagrams, *Phys. Rev. D*, 1978, 18, 1939-55.
- [28] Arquès D., Béraud J.-F., Rooted maps on orientable surfaces, Riccati's equation and continued fractions, *Discr. Math.*, 2000, 215, 1-12.
- [29] Arquès D., Relations fonctionelles et denombremant des cartes pointees sur le tore, *J. Combin. Theory, Series B*, 1987, 43, 253-274.
- [30] Van Houcke K., Werner F., Kozik E., Prokof'ev N., Svistunov, B., Ku M.J.H., Sommer A.T., Cheuk L.W., Schiroztek A., Zwierlein M.W., Feynman diagrams versus Fermi-gas Feynman emulator, *Nat. Phys.*, 2012, 8, 366-370.
- [31] Drischler C., Hebelker K., Schwenk A., Chiral interactions up to N3LO and nuclear saturation, 2017, arXiv: 1710.08220.
- [32] Furry W.H., A Symmetry Theorem in the Positron Theory. *Phys. Rev.*, 1937, 51, 125.
- [33] Tutte W.T., A census of slicings, *Can. J. Math.*, 1962, 14, 708-722.
- [34] Tutte W.T., A census of planar maps, *Can. J. Math.*, 1963, 15, 249-271.
- [35] Tutte W.T., On the enumeration of planar maps, *Bulletin of the Amer. Math. Soc.*, 1968, 74(1), 64-74.
- [36] Brown W.G., Enumerative problems of linear graph theory (PhD Thesis), University of Toronto, 1963
- [37] Brown W.G., On the number of nonplanar maps. *Memoirs of the American Mathematical Society*, 1966, 65, 1-42.
- [38] Brown W.G., Tutte, W.T., On the enumeration of rooted non-separable planar maps, *Can. J. Math.*, 1964, 16, 572-577.
- [39] Walsh T.R., Lehman A.B., Counting rooted maps by genus I, *J. Combin. Theory, Series B*, 1972, 13, 192-218.
- [40] Walsh T.R., Lehman A.B., Counting rooted maps by genus II, *J. Combin. Theory, Series B*, 1972, 13, 122-141.
- [41] Walsh T.R., Lehman A.B., Counting rooted maps by genus III, *J. Combin. Theory, Series B*, 1975, 18, 222-259.
- [42] Cairns S.S., *Introductory Topology*, Ronald Press, New York, 1961
- [43] Bender E.A., Canfield, E.R., The number of degree restricted rooted maps on the sphere, *SIAM J. Discr. Math.*, 1994, 7, 9-15.
- [44] Bender E.A., Canfield E.R., The asymptotic number of rooted maps on a surface. *J. Combin. Theory, Series A*, 1986, 43, 244-257.
- [45] Bender E.A., Canfield E.R., Robinson R.W., The enumeration of maps on the torus and the projective plane, *Can. Math. Bulletin*, 1988, 31, 257-271.
- [46] Bender E.A., Canfield, E.R., The number of rooted maps on an orientable surface, *J. Combin. Theory, Series B*, 1991, 53, 293-299.
- [47] Touchard J., Sur une probleme de configurations et sur les fractions continues, *Can. J. Math.*, 1952, 4, 2-25.
- [48] Courcelle B., Dussuax V., Map genus, forbidden maps, and monadic second-order logic, *Electr. J. Combin.*, 2002, 9(1), R40, 27.

- [49] Krikun M.A., Malyshev V.A., Asymptotic number of maps on compact orientable surfaces, *Discr. Math. Applic.*, 2001, 11, 145-255.
- [50] Krikun M.A., Malyshev V.A., Random Boundary of a Planar Map, In: D. Gardy, A. Mokkaedem (Eds.) *Trends in Mathematics, Mathematics and Computer Science*, BirkHauser, 2002, 83-93.
- [51] Krikun M.A., Malyshev V.A., *Asymptotic Combinatorics with Applications to Mathematical Physics*, Kluwer, 2002
- [52] Schaeffer G., *Bijjective Census and Random Generation of Eulerian Planar Maps with Prescribed Vertex Degrees*, *The Electr. J. Combin.*, 1997, 4(1), n.R20
- [53] Schaeffer G., Poulalhon, D., A note on bipartite Eulerian planar maps, 2002, www.lix.polytechnique.fr/~schaeffe/Biblio/PoSc02b.ps
- [54] Schaeffer G., *Conjugaison d'arbres et cartes combinatoires aleatoires* (PhD thesies), University Bordeaux I, 1998
- [55] Jackson D.M., Visentin, T.I., *An atlas of the smaller maps in orientable and nonorientable surfaces*, Chapman & Hall/CRC, 2000
- [56] Yanpei L., *Enumerative Theory of Maps*, Kluwer Academic Publishers, 2000
- [57] Dodson C.T., Parker P.E., *A user's guide to algebraic topology*, Kluwer Academic Publishers, 1997
- [58] Fetter A.L., Walecka J.D., *Quantum theory of many particle systems*, McGraw-Hill Publishing Company, 1971
- [59] Dickhoff W.H., Van Neck D., *Many-Body Theory Exposed! Propagator description of Quantum Mechanics in Many-Body Systems*, World Scientific Publishing Company, 2006
- [60] Stefanucci G., Van Leeuwen R., *Non-Equilibrium Many-Body Theory of Quantum Systems*, Cambridge Univ. Press, 2013
- [61] Carsten T., The graph genus problem is NP-complete, *J. Algorithms*, 1989, 10(4), 568-576.
- [62] Kang J.S., Dynamical symmetry breaking of U(N)-symmetric gauge theory in the 1/N expansion, *Phys. Rev. D*, 1976, 14, 1587-1601.
- [63] Gross D.J., Mikhailov A., Roiban R., A calculation of the plane wave string Hamiltonian from N = 4 super-Yang-Mills theory, *J. High Energy Phys.*, 2003, 0305, 025.
- [64] Nayak C., *Many Body Physics*, University of California, Los Angeles, 1999
- [65] Schwarz J.H., Update on String Theory, 2003, [arXiv:astro-ph/0304507v1](https://arxiv.org/abs/astro-ph/0304507v1).
- [66] Wick G.C., The Evaluation of the Collision Matrix, *Physical Review*, 1950, 80, 268.
- [67] Ursell H.D., The evaluation of Gibbs' phase-integral for imperfect gases, *Proceedings of the Cambridge Philosophical Society*, 1927, 23, 685.
- [68] Mayer J.E., Mayer M.G., *Statistical Mechanics*, John Wiley and Sons, New York, 1941

Appendix A

Building Feynman diagrams

Let us build the Feynman diagrams for the single-particle Green's function at the m -th order in perturbation theory. For any given diagram there is an identical contribution from all similar diagrams that merely differ in the permutation of the space-time labels in the interaction Hamiltonian.

In m -th order there are $m!$ ways of choosing the sequence of the interaction Hamiltonians by applying Wick's theorem [66]. All of these terms give the same contribution to the Green's function, so that we can count each diagram just once and cancel the factor $\frac{1}{m!}$ in formula (4). Note that this result is true only for the connected diagrams, where the external points x and y are fixed.

Let us now revisit the rules for building all the Feynman diagrams contributing to single-particle Green's function.

1. Draw all *topologically distinct* connected diagrams with m interaction lines and $2m + 1$ oriented lines representing Green's functions. This procedure can be topologically simplified by observing that a Fermion line either closes on itself or runs continuously from y to x . Each diagram represents all the $m!$ different possibilities of ordering the set of space variables. If there is a problem concerning the precise meaning of topologically distinct diagrams, Wick's theorem can always be used to verify the enumeration.
2. Label each vertex with a four-dimensional space-time point.
3. Each solid line between the two points represents a free single-particle Green's function.
4. Each dashed line represents an interaction (more precisely its matrix element in spin-space).
5. Integrate over all internal space and time variables.
6. There is a spin matrix product along each continuous fermion line, including the potential at each vertex.
7. Affix a sign factor $(-1)^l$, where l is the number of closed fermion loops in the diagram.¹⁴

¹⁴ The overall sign of the various contributions appearing in the diagrams is determined as follows: every time a fermion line closes on itself, the term acquires an extra minus sign.

8. To compute $G(x, y)$ assign a factor $\left(\frac{i}{\hbar}\right)^m = (-i) \left(-\frac{i}{\hbar}\right)^m i^{2m+1}$ to each m -th order term.

The foregoing statements provide a unique prescription for drawing and evaluating all Feynman diagrams that contribute to the Green’s function in coordinate space. Each diagram corresponds to an analytic expression that can be now written down explicitly with the Feynman rules. The calculation of Green’s function becomes then a relatively automatic although non-trivial process.

Appendix B

First and second-order diagrams

As an example of the Feynman rules, we show the complete first-order contribution to the Green’s function in Figure A1.

The corresponding second-order contribution requires more work and, according to many-body textbooks, we can assert that there are 10 second-order Feynman diagrams (see Figure A2).

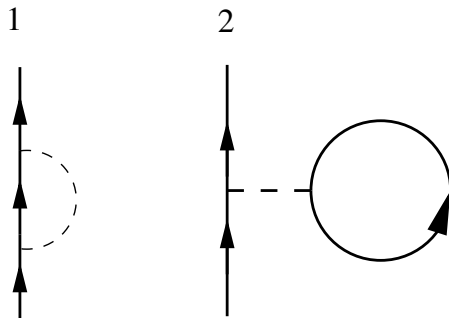


Figure A1: First-order diagrams.

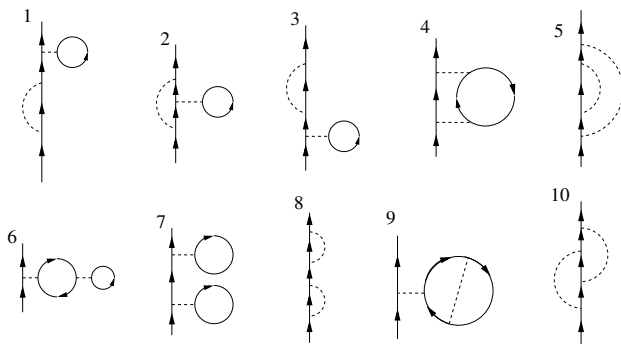


Figure A2: Second-order Feynman diagrams [58].

Historically speaking, Feynman diagrams are not the first graphical approach to a complex physics problem. First efforts were made in the integration of dynamical systems in the realm of thermodynamics and statistical mechanics. An interesting example of this approach is the one developed by Ursell and Mayer [67, 68] in order to determine the partition function of an interacting gas, known as the *cluster expansion*.

Appendix C

Third-order diagrams

Even though the number of Feynman diagrams for the electron propagator has been found out many years ago, it seems that a graphical enumeration of third-order diagrams (or beyond) has never been done. Nevertheless, in order to make a comparison with rooted maps, which are essential in characterizing the topological properties of orientable surfaces, the graphical identification and enumeration of the diagrams may be an useful tool. Thus we looked both to the *number* of Feynman diagrams at third-order and to the *structure* of each diagram. For this purpose, we have devised an easy procedure for drawing all topologically distinct Feynman diagrams at *any* order. First of all we built the 10 second-order diagrams starting from the “shell” and the “tadpole” diagrams of first order. This way we can enumerate the first three numbers of the puzzling “quantum many-body theory integer sequence” (perturbation order N versus number of quantum many-body theory diagrams).

We show the building procedure (see Figure A3) applied to first-order diagrams in such a way as to obtain the (already known) second-order ones and in general to show how to apply it for higher orders:

1. Consider the “shell” diagram.
2. We draw *one* bold point in the middle of a propagation line: it will become the tadpole tail of a new second-order diagram; of course we can draw a bold point in three different positions¹⁵, so that we should built three new different second-order quantum many-body theory diagrams, starting from the first-order shell one.

¹⁵ Often we refer to the set of segments representing Green functions and connecting the initial and final vertices straightforwardly as the *root line*.

3. Then we have to put *two* bold points on any propagation line, and they will become the shell extremes of a new second-order diagram.
4. Repeat steps 1,2 and 3 starting with the “tadpole” diagram.

The procedure is the same for higher orders: to obtain the m th-order diagrams one has to apply it to every diagram of the $(m - 1)$ th-order. The result of our building procedure applied to the first-order diagram of Figure A1 are the 10 second-order diagrams of Figure A2. For the third-order, we have to start from the 10 distinct diagrams of the second-order, and so on...

This way, we can build all Feynman diagrams: we notice that *the extreme of an interaction line can only be attached to a propagation line, hence to the “points” systematically added in the lower order diagram*. Obviously similar diagrams may arise from this procedure: therefore at the end of the process, we have to discard *topologically equivalent* diagrams, which are such if there exist a continuous transformation in the plane between each part of the two diagrams (see Figure A3). The physical meaning

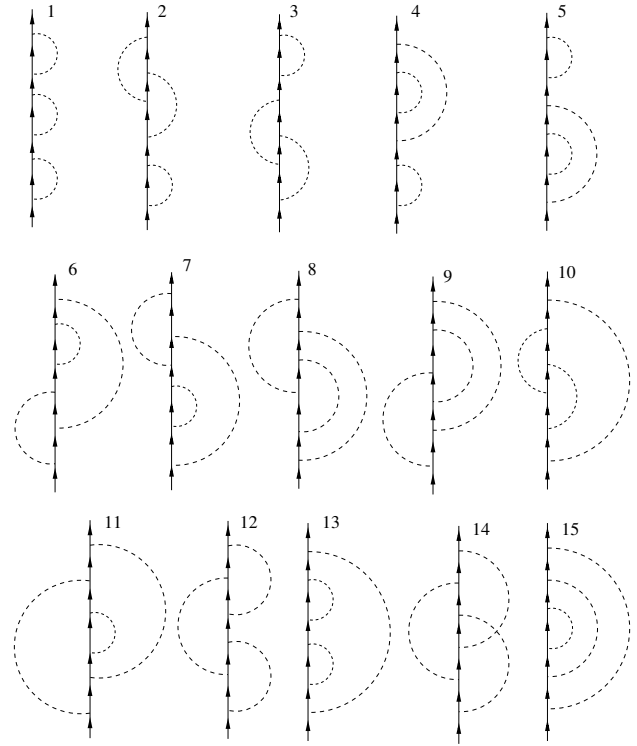


Figure A4: “Shells” Feynman diagrams of third-order. Interaction vertices are added only on the root of shells diagrams of preceding order. These diagrams are simply computed by the Touchard formula: if m is the perturbative order (*i.e.* number of shells), the number of shells-diagrams is $(2m - 1)!!$.

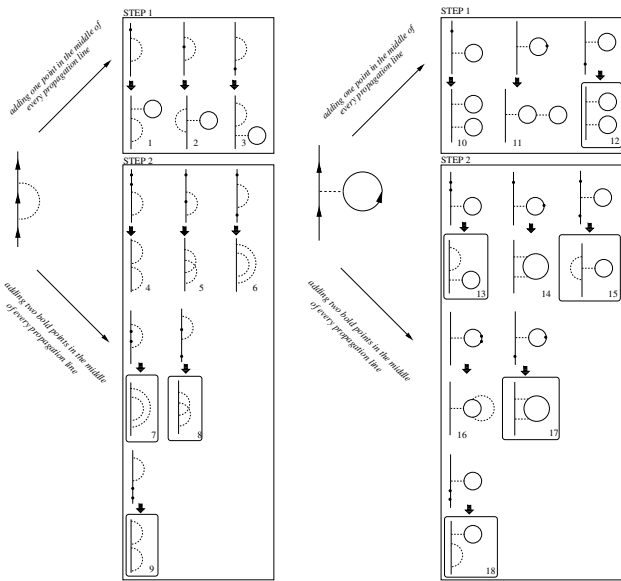


Figure A3: Examples of the graphical construction for the second-order Green’s function diagrams, starting from the two diagrams at first-order: “Shell” and “Tadpole”. In step 1 we put *one* bold point in the middle of a propagation line; then we add a *tadpole* where we have just put that point. In step 2 we add, analogously, *two* bold points and connect them with a dashed line representing a new *shell* interaction. Obviously these points must be put in every available position. We thus obtain 18 diagrams but it is easy to observe that 8 of them (the ones shown inside rectangular boxes) appear twice and must be discarded as topologically equivalent to other diagrams (in agreement with Feynman rule number 1).

of this rules directly stems from the Wick’s Theorem [66] applied to the propagator.

We now show the results of the above established procedure for building all third-order diagrams. As expected, we have obtained 74 different diagrams: 15 of them - we loosely refer to them as to “shells” diagrams, - can be enumerated by a very easy formula since they contain only shells and no tadpoles¹⁶. At the m -th perturbative order their number is:

$$F_{shell}(m) = (2m - 1)!! = 1 \cdot 3 \cdot 5 \cdot 7 \dots$$

This formula was extracted by Touchard in an old strictly mathematical work [47], and recently rediscovered by several physicists among whom Kuchinskii [21].

Checking all topologically equivalent diagrams, we found that there exist 42 additional diagrams which are obtained by adding a shell or a tadpole in every available position right in the root line (see Figures A5 and A5).

¹⁶ In this class of graphs, interaction vertices lie on the same propagation line directly connecting the initial and final vertices of the many-body Green’s function diagram.

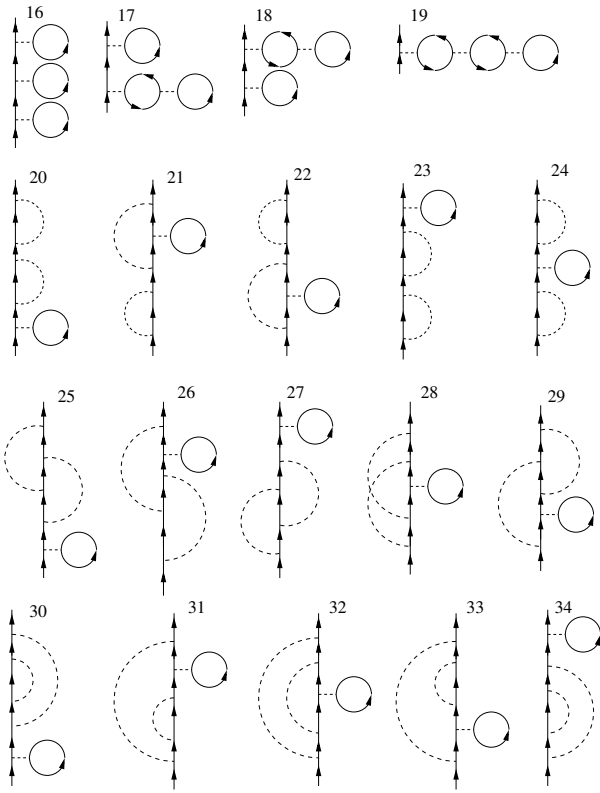


Figure A5: (a) Third-order Feynman diagrams. (continued)

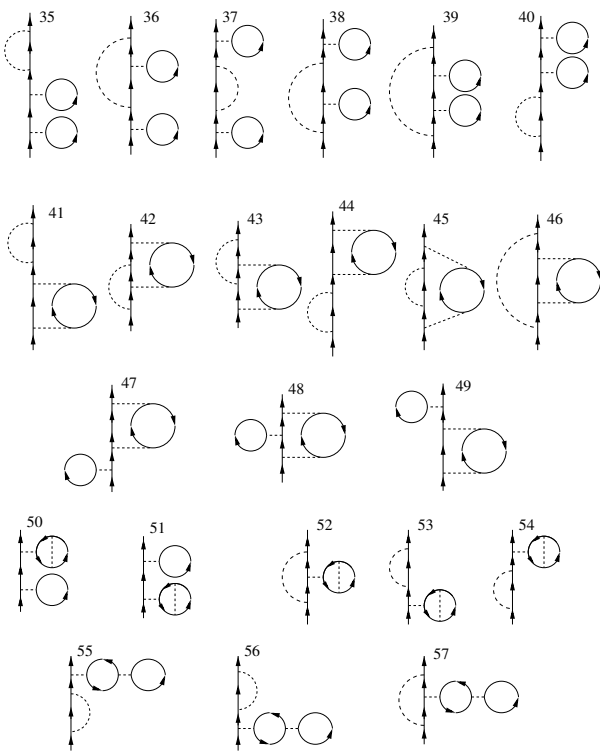


Figure A5: (b) Third-order Feynman diagrams (continued).

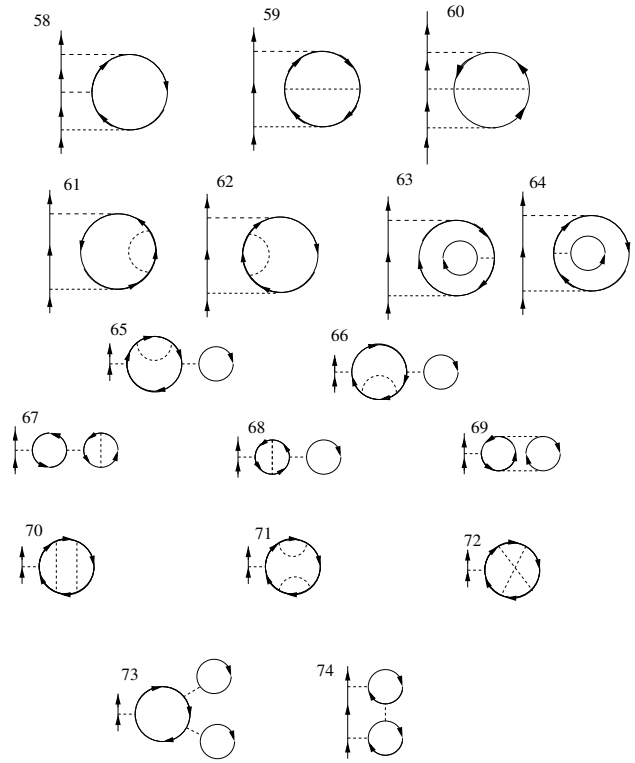


Figure A5: (c) Third-order Feynman diagrams (continued).

Moreover there are 18 diagrams derived from second-order diagrams by adding a tadpole (or a shell) onto a tadpole - or a shell between the root line and a tadpole (Figure A5). The complete set of the single-particle Green's function Feynman diagrams at third-order (in addition to the ones in Figure A4) is illustrated in Figures A5a, A5b and A5c.